Am J Transl Res 2021;13(9):10262-10275
www.ajtr.org /ISSN:1943-8141/AJTR0133893

Original Article

LncRNA MALAT1 promotes breast cancer progression by sponging miR101-3p to mediate mTOR/PKM2 signal transmission

Jianqiang Shao, Qin Zhang, Peng Wang, Zunyi Wang

Department III of Thyroid & Breast, Cangzhou Central Hospital, Cangzhou 061000, Hebei, China

Received April 4, 2021; Accepted July 6, 2021; Epub September 15, 2021; Published September 30, 2021

Abstract: Breast cancer (BC) is a common malignant tumor in women and exhibits a poor prognosis. This study examined the role and underlying mechanisms of long non-coding RNA (lncRNA), metastasis-associated lung adenocarcinoma transcript 1 (MALAT1) in BC pathogenesis. The MALAT1 expression levels in BC cells and tissues were measured using quantitative reverse transcription-polymerase chain reactions. CCK-8 kits and wound healing and transwell assays were used to evaluate the cell growth, invasion, and migration of BC. Bioinformatics and dual-luciferase reporter analyses were conducted to identify MALAT1's potential targets. The protein levels in the mTOR/PKM2 pathway were assessed using Western blot analyses. The MALAT1 overexpressions in the BC tissues and cells were considered to be a predictor of poor prognosis. Therefore, MALAT1 downregulation significantly inhibited BC progression, including cell growth, invasion, and migration. MALAT1 was anticipated to be an miR-101-3p target according to the dual-luciferase reporter gene assay results. The miR-101-3p levels were indirectly proportional to the MALAT1 expressions and the suppressed BC cells. Additionally, the mTOR/PKM2 pathway was directly targeted by miR-101-3p. MALAT1 overexpression significantly decreased the miR-101-3p gene levels and increased the mTOR/PKM2 pathway protein expressions. This miR-101-3p inhibition blocked MALAT1. These findings suggest that lncRNA MALAT1 is related to BC pathogenesis using the miR101-3p/mTOR/PKM2 pathway and is a potential therapeutic target.

Keywords: MALAT1, miR-101-3p, breast cancer, mTOR/PKM2 pathway

Introduction

Breast cancer (BC) is a common malignant tumor in women and a major cause of cancer-related mortality [1]. Despite therapeutic advances in local and systemic therapy, BC remains a lethal disease [2-4]. Patients with advanced BC have a 5-year survival rate as low as 22% [5]. However, the molecular mechanisms of BC progression and metastasis leading to the loss of normal biological function are still unclear. Thus, the mechanism of BC progression must be clarified to discover a safe and effective treatment for BC.

Functional genomic analyses show that less than 2% of the genes encode proteins in the genome, and the remaining 98% of the genes are non-coding RNAs (ncRNAs), which can be categorized into two types, namely long ncRNAs (lncRNA) and small ncRNAs. Small ncRNAs include small interfering RNAs (siRNAs) and microRNAs (miRNAs) [6]. LncRNAs are defined as transcripts longer than 200 nucleotides, and several lnRNAs are expressed as biomarkers in diseases such as malignancies [7]. LncRNAs play a major role in cellular processes including the cell cycle, migration, invasion, metastasis, and apoptosis and regulate biological functions in transcriptional and post-transcriptional gene expression [8-13]. lncRNA metastasis-associated lung adenocarcinoma transcript 1 (MALAT1) has a high conservation degree in mammalian species and is abundantly expressed in normal tissues, mediating pre-mRNA splicing and gene expression [14]. Clinical studies have reported MALAT1 upregulation in malignancies such as BC [15, 16]. MALAT1 overexpression in BC promotes proliferation, motility, angiogenesis, and metastasis

[15]. Additionally, MALAT1 has been found to be a prognostic marker for poor clinical overcomes with regards to overall survival and metastasis-free survival in BC patients [17, 18]. However, the biological mechanism of MALAT1 in BC patients is still unclear.

The present study aimed to determine the biological function of MALAT1 and explore the candidate treatment for BC. In this study, we evaluated the MALAT1 levels in BC cells and tissues and investigated the role of MALAT1 function in BC cell tumorigenesis.

Materials and methods

Tissue samples and cell lines

This study was conducted using 71 intraoperative tumor specimens from BC patients and matched normal specimens (> 5 cm away from the tumor tissue edge). Only female patients with an average age of 45 ± 8 years were enrolled in the study. According to the American Joint Committee on Cancer (AJCC) 8th edition, 21, 35, and 15 of the patients were in stages I, II, and III, respectively. Patients pathologically diagnosed with invasive BC and with no history of preoperative radiotherapy, chemotherapy, or endocrine therapy, no distant metastasis, and complete follow-up information were included in the study. Patients not conforming to the inclusion criteria and those with additional cancers or disorders were excluded from the study. The five-year survival rates of the BC patients were recorded, and overall survival was defined as the time between diagnosis and death or the last follow-up. Informed consent was obtained from all the participants. The study was conducted according to the Declaration of Helsinki after we obtained an institutional ethics clearance (No. CZ2018101201).

For this study, BC cells (MDA-MB-231, MCF-7, BT474, and MDA-MB-453) and non-carcinoma MCF-10A breast epithelial cells were provided by the Cell Bank of the Chinese Academy of Sciences (Shanghai, China) and cultured in Dulbecco's Modified Eagle Medium (DMEM) containing 10% fetal bovine serum (FBS) at 37°C under 5% CO_2. The medium was changed at two-day intervals. The Cell passage was conducted at 80%-90% density.

Cell transfection

MDA-MB-231 and MCF-7 cells (5,000/well) at the logarithmic phase were inoculated in the 6-well culture plates for another 24 h. Cells reaching 60%-80% confluence were collected for the transfection. siRNA-targeted MALAT1 (si-MALAT1 #1: 5'-CACCGCTGTGGAGTTCTTAAATATCTTCAAGAGAGATATTTAAGAACTCCACAGCTTTTTTG-3', #2: 5'-GAGCAAAGGAAGUGGCUUATT-3'), the siRNA-scrambled controls (si-NC: 5'-UUCUCCGAACGUGUCACGUTT-3'), pcDNA3.1-MALAT1 (OE-MALAT1 group), pcDNA3.1-NC (OE-NC group), the miR-101-3p mimics, the miR-101-3p inhibitor, and NC were obtained for the cell transfection using lipofectamine 2000 (Invitrogen, CA, USA).

Quantitative reverse transcription-polymerase chain reaction

Trizol kits (Invitrogen, CA, USA) were used to extract the total tissue and the cellular RNAs. Then, the RNA was converted into cDNA using PrimeScript RT reagent kits with gDNA Eraser (Invitrogen, CA, USA) through reverse transcription. Additionally, the cDNAs were synthesized from the RNA of the miRNA using miRNA cDNA First Strand Synthesis (GenePharma Co. Ltd. Shanghai, China). The polymerase chain reactions (PCR) were conducted using miRcute miRNA Fluorescence Quantitation Kits (GenePharma Co. Ltd., Shanghai, China) on an Applied Biosystems 7300 (Thermo Scientific, Waltham, USA) or a FastStart Universal SYBR Green master mix (Invitrogen, CA, USA), with glyceraldehyde 3-phosphate dehydrogenase as the endogenous reference gene to quantify the mRNA or lncRNA and U6 as endogenous references to measure the miRNA. The relative expressions were determined according to the $2^{-\Delta\Delta Ct}$ values. All the experiments were performed three times with six duplicates. **Table 1** lists all the primers used.

The cell proliferation assays

We used Cell Counting Kit-8 (CCK-8) assays (Beyotime, Shanghai, China) to evaluate the cell proliferation. The cells at the logarithmic growth stage (1 × 10^6/well) were inoculated into 96-well plates, followed by culturing in 100 μL of culture medium in a standard cell constant temperature incubator for 6 h. At 24, 48, 72, and 96 h, 10 μL of CCK-8 solution was added to

Table 1. Sequences of all the primers utilized in this study

Gene	Sequences of primers (5'-3')
MALAT1	5'-GCGACGAGTTGTGCTGCTATCT-3' (forward) 5'-ACACTGCTCTGGGTCTGCTTTT-3' (reverse)
GAPDH	5'-GAGTCAACGGATTTGGTCGT-3' (forward) 5'-CATGGGTGGAATCATATTGGA-3' (reverse)
U6	5'-TCCGATCGTGAAGCGTTC-3' (forward) 5'-GTGCAGGGTCCGAGGT-3' (reverse)
miR-101-3p	5'-TCCGAAAGTCAATAGTGTC-3' (forward) 5'-GTGCAGGGTCCGAGGT-3' (reverse)
PKM2	5'-ACTCGGGCTGAAGGCAGTGA-3' (forward) 5'-TGTGGGGTCGCTGGTAATGG-3' (reverse)
mTOR	5'-ATGACGAGACCCAGGCTAAG-3' (forward) 5'-GCCAGTCCATGCCATCAG-3' (reverse)

each well, and the cells were incubated for another 2 h. An automated microplate reader (BioTek Instruments, Winooski, USA) was used to determine the absorbance (OD) values at 450 nm and to calculate the cell proliferation in each group. The experiment was repeated at least three times.

Transwell assays

Transwell chambers (Corning, New York, USA) were used to assess the cell invasion. A sterile 24-well plate was placed in the transwell cell chamber, and 80 μL of matrix glue was placed in the cell chamber at a ratio of 1:10. The 24-well plate with matrix glue was placed in the cell constant temperature incubator for 4 h to allow it to settle. Then, 600 μL of DMEM containing 10% FBS was added and the cells were cultured for a period of 24 h. Thereafter, the chamber bottom was cleaned twice with phosphate-buffered saline (PBS), and the cells that had not penetrated onto the internal chamber surface were wiped with a cotton rod. The cells that had passed the internal chamber surface were fixed with 4% paraformaldehyde, and after 10 min, the cells were stained with 0.5% crystal violet (Biosharp, Anhui, China) for 15 min. Five fields of view were randomized to count the number of cells under a microscope (Olympus, Tokyo, Japan). All the experiments were conducted in triplicate.

Scratch assays

The cells were inoculated in the 6-well plates (5×10^5/well) and incubated for 24 h at 37°C. When the cells had grown to 80% confluency, a sterile micropipette tip was used to create wounds by scratching along the midline of the plate. Then, the floating cells were washed out with 2% PBS, followed by the addition of some serum-free medium to each well. At 0 and 24 h, the scrape line of the wound healing was observed, and an inverted microscope (Olympus, Tokyo, Japan) was used to evaluate the wound dimensions in five random fields.

Dual-luciferase reporter gene assays

We used the Starbase 2.0 database (http://starbase.sysu.edu.cn/) to predict the relationship between MALAT1 and the miRNA targets. Additionally, the TargetScan database (http://www.targetscan.org/vert_72/) was used to predict the relationship between mTOR and the miRNA targets, and dual-luciferase reporter assays were used to assess the binding relations. The pmirGLO luciferase reporter vector was used to construct the pmirGLO-MALAT1 (MALAT1-Wt) or pmirGLO-mTOR (mTOR-Wt) vector at 3'UTR of the luciferase open reading frame, which was cloned with full length genes and without CA-repeats. Additionally, the MALAT1 or mTOR mutant miR-101-3p binding site was constructed using the pmirGLO-MALAT1-Mut (MALAT1-Mut) vector and the pmirGLO-mTOR-Mut (mTOR-Mut) vector. The cells were cotransfected with 400 ng luciferase vector and NC or miR-101-3p mimics (50 ng) using lipofectamine 3000. At 48 h post-transfection, we used dual-luciferase assay kits (Promega, Shanghai, China) to measure the Renilla and firefly luciferase activities, with the activity of the firefly luciferase being normalized to that of Renilla. The results were represented as a fold induction compared with the NC group.

Western blotting

The present study extracted the total proteins using RIPA lysis buffers (Invitrogen, CA, USA). The protein bands were separated using 10% SDS-PAGE, following an examination of the protein concentrations using a BCA kit (Beyotime, Shanghai, China), before being transferred onto a poly (vinylidene fluoride) (PVDF) membrane (EMD Millipore, Billerica, USA). Then, 10% nonfat milk was used to block the membrane for 2

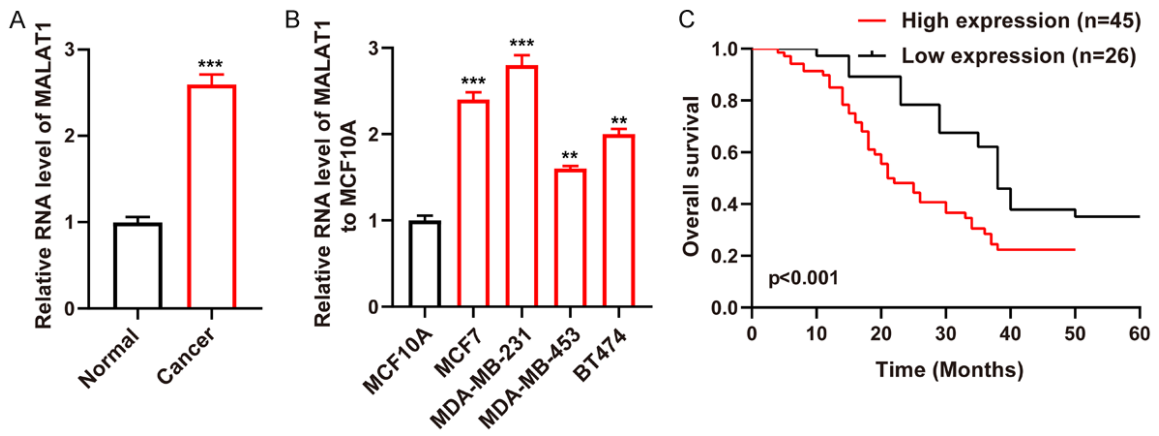

Figure 1. The MALAT1 expressions in the BC cells and tissues. A. The MALAT1 levels in the 71 paired BC and matched non-BC samples were evaluated using qRT-PCR. Compared to the normal group, $^{***}P < 0.001$. B. The MALAT1 levels in the BC cells and non-carcinoma MCF-10A breast epithelial cells. Compared to the MCF10A cells, $^{**}P < 0.01$, $^{***}P < 0.001$. C. High and low MALAT1 levels expressing the total survival rates for the BC cases using a Kaplan-Meier survival curve analysis.

h under at the temperature, and then the membrane was incubated overnight using the corresponding primary antibodies at 4°C. HRP-labelled secondary antibody (1:10000, Jackson ImmunoResearch, West Grove, PA) was used to further incubate the membrane for another 1 h at the ambient temperature. All the primary antibodies used were rabbit anti-β-actin polyclonal antibodies (pab, 1:2000, ProteinTech, Wuhan, China), rabbit anti-mTOR, and anti-PKM2 pab (1:2000, CST, MA, USA). Immunoreactive proteins were then developed using enhanced chemiluminescence (ECL) and detection reagents (Millipore, Massachusetts, USA). The densitometry was conducted using ImageJ software.

Statistical analysis

The results are displayed as the mean ± standard deviation and were collected in three independent experiments. The statistical analysis was conducted using GraphPad prism 6.0. The post hoc comparisons were performed for the data among multiple groups using Bonferroni tests. Student's *t* tests were conducted to investigate the differences between two groups. Log rank tests were used to create the Kaplan-Meier survival curves, and Spearman's correlation analyses were used for displaying the associations between two variates. A *P* value < 0.05 was considered statistically significant.

Results

MALAT1 upregulation predicted the dismal prognostic outcomes of the BC patients

The present study evaluated the role of MALAT1 in BC pathogenesis by analyzing its levels in BC and in matched normal samples. The MALAT1 expression was higher in the BC samples than in the normal adjacent tissues (**Figure 1A**). Additionally, the MALAT1 levels were higher in the BT474, MCF7, MDA-MB-453, and MDA-MB-231 cells than in MCF-10A (**Figure 1B**). The patients were classified into the upregulation (n = 45) and downregulation (n = 26) groups according to the median MALAT1 expression to assess the relationship between the clinicopathological features of the BC patients and the MALAT1 levels. Our Kaplan-Meier analyses indicated that survival was poorer in the MALAT1 upregulation group than in the downrugulation group (**Figure 1C**).

MALAT1 knockdown inhibited the BC cell proliferation, invasion, and migration

To clarify the effect MALAT1 on the BC cells, we established a MALAT1 knockdown model through a transfection with siRNA against the MALAT1 plasmid in the BC cells. MDA-MB-231 and MCF-7 cells were selected to explore the effect of MALAT1 on the BC cells. Therefore, the si-MALAT1 transfection significantly decreased the MALAT1 expression (**Figure 2A**). The

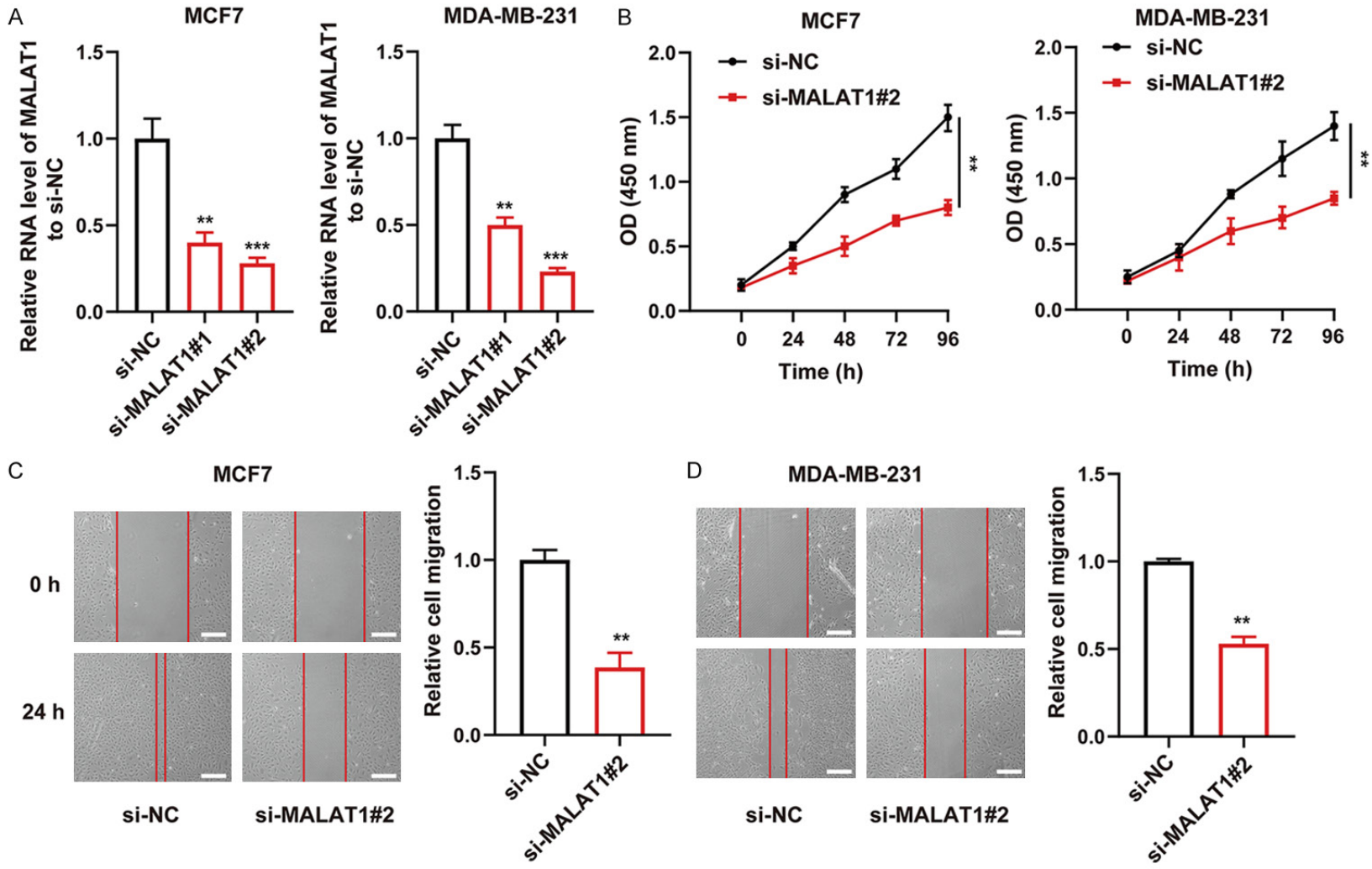
A
MCF7
Relative RNA level of MALAT1 to si-NC
1.5
1.0
0.5
0.0
**
***
si-NC
si-MALAT1#1
si-MALAT1#2
MDA-MB-231
Relative RNA level of MALAT1 to si-NC
1.5
1.0
0.5
0.0
**
***
si-NC
si-MALAT1#1
si-MALAT1#2
B
MCF7
si-NC
si-MALAT1#2
OD (450 nm)
2.0
1.5
1.0
0.5
0.0
**
0
24
48
72
96
Time (h)
MDA-MB-231
si-NC
si-MALAT1#2
OD (450 nm)
2.0
1.5
1.0
0.5
0.0
**
0
24
48
72
96
Time (h)
C
MCF7
0 h
24 h
si-NC
si-MALAT1#2
Relative cell migration
1.5
1.0
0.5
0.0
**
si-NC
si-MALAT1#2
D
MDA-MB-231
si-NC
si-MALAT1#2
Relative cell migration
1.5
1.0
0.5
0.0
**
si-NC
si-MALAT1#2

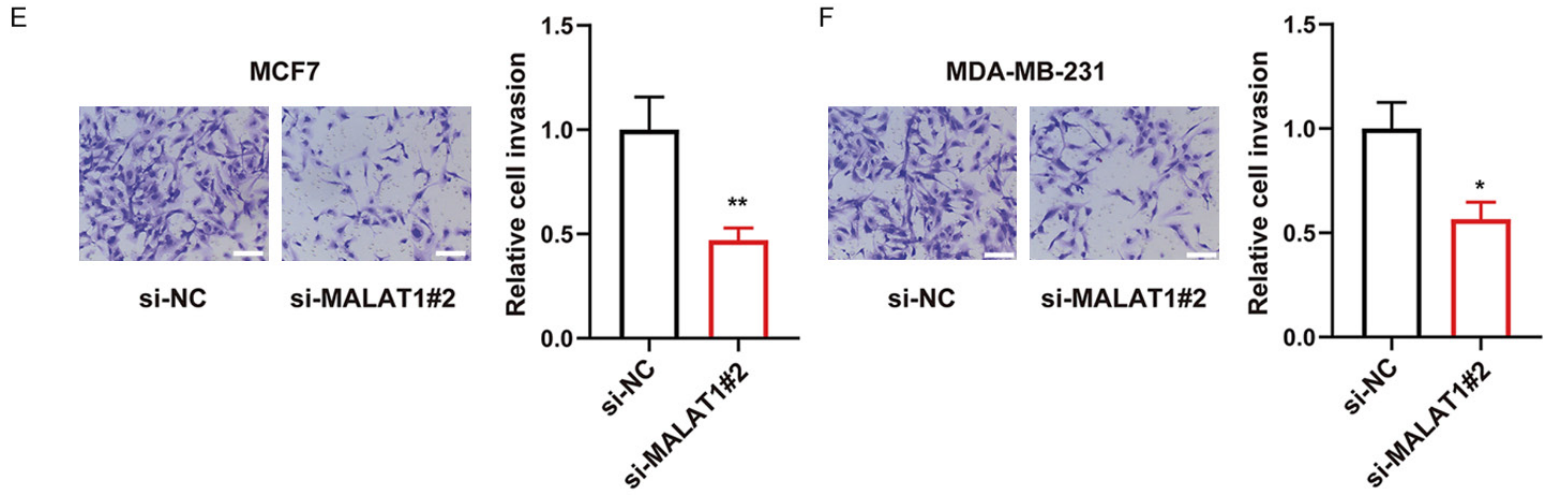

Figure 2. Decreased MALAT1 expression inhibits BC cell proliferation, invasion, and migration. A. MDA-MB-231 and MCF-7 cells subjected to si-NC, si-MALAT1#1, and si-MALAT1#2 transfection, MALAT1 levels measured using qRT-PCR. B. Role of si-MALAT1#2 in BC cell proliferation determined using CCK8 assays. C and D. Migration of the si-MALAT1#2 transfected BC cells analyzed using scratch assays (scale bar = 500 μm, magnification × 40). E and F. Cell invasion of the si-MALAT1#2 transfected BC cells measured using transwell assays (magnification × 200, scale bar = 100 μm). Compared to the si-NC group, $^{*}P < 0.05$, $^{**}P < 0.01$, $^{***}P < 0.001$.

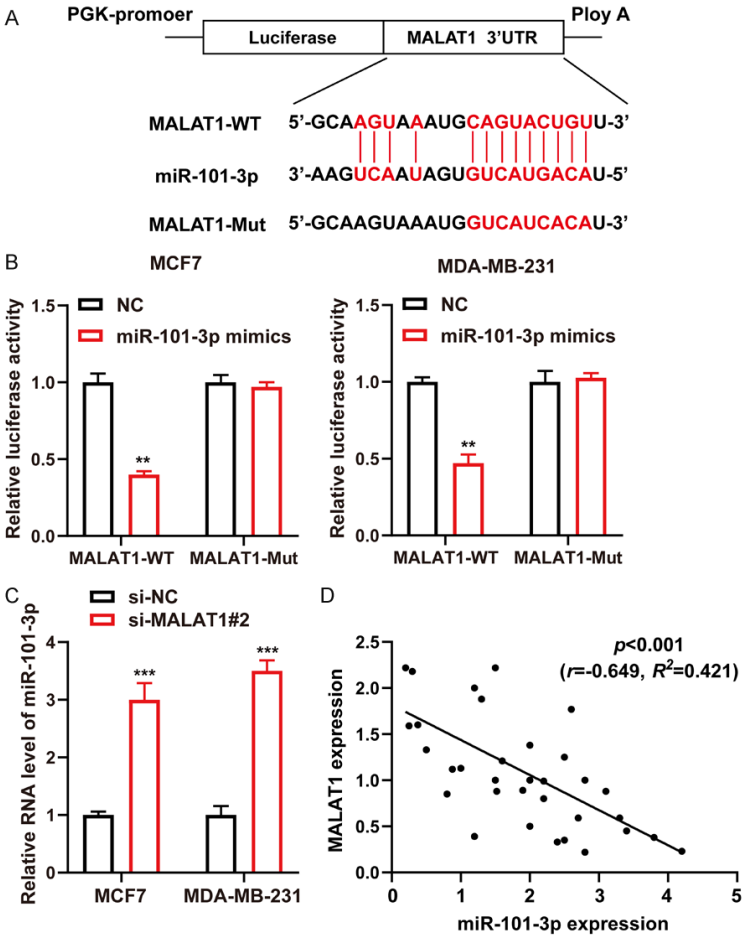

Figure 3. The association between MALAT1 and miR-101-3p. A. The plasmids with the MALAT1-Mut and MALAT1-WT luciferase reporter cloned by mutating the putative miR-101-3p binding site in MALAT1. B. Dual-luciferase assays were used to verify the targeted relationship between MALAT1 and miR-101-3p. Compared to the NC group, $^{**}P < 0.01$. C. miR-101-3p level in the si-MALAT1#2 transfected cells assessed using qRT-PCR. Compared to the si-NC group, $^{***}P < 0.001$. D. The association of the miR-101-3p expression with the MALAT1 expression in the BC clinical samples identified using Spearman's correlation.

MALAT1 knockdown significantly inhibited the cell proliferation at 24, 48, 72, and 96 h through the CCK8 assay by a comparison with the si-NC transfection cells (**Figure 2B**). Scratch and transwell assays were performed to investigate the mechanism by which the MALAT1 knockdown affects the BC cell invasion and migration. Therefore, the BC cell migration (**Figure 2C**, **2D**) and invasion (**Figure 2E**, **2F**) were significantly lower in the si-MALAT1 group than in the si-NC group.

MiR-101-3p was the direct target of MALAT1 in the BC cells

We predicted the MALAT1 target miRNAs using the Starbase 2.0 database to explore the possible mechanisms of the malignant biological activity by which MALAT1 regulates BC cells. Therefore, miR-101-3p served as a possible target, and the binding site is illustrated in **Figure 3A**. The miR-101-3p mimics reduced the luciferase activities in the BC cells under MALAT1-WT transfection, but the miR-101-3p mimics did not significantly affect the luciferase activity of the MALAT1-Mut transfected BC cells (**Figure 3B**). The miR-101-3p levels in the BC cells exposed to the si-NC or si-MALAT1 transfections were also explored; the levels were found to be significantly elevated in the si-MALAT1 cells compared with the levels in the si-NC cells (**Figure 3C**). Additionally, our Spearman's correlation analysis showed that the MALAT1 levels were indirectly proportional to the miR-101-3p levels (**Figure 3D**). Furthermore, miR-101-3p might be a MALAT1 direct target in BC cells.

MiR-101-3p overexpression inhibited BC cell growth, invasion, and migration

Following the NC or miR-101-3p mimic treatment, the miR-101-3p levels were elevated significantly within the MDA-MB-231 and MCF-7 exposed to the miR-101-3p mimics transfection. However, an increase in the miR-101-3p level was not observed in the NC group (**Figure 4A**). Additionally, the miR-101-3p mimics significantly suppressed the cell growth (**Figure 4B**), migration (**Figure 4C**, **4D**), and invasion compared with the NC group (**Figure 4E**, **4F**).

The MALAT1 knockdown targeting miR-101-3p inhibits the mTOR/PKM2 pathway in the BC cells

The TargetScan database was used to predict the miR-101-3p downstream targets to further improve the possible molecular mechanism by which MALAT1 regulates the malignant biologi-

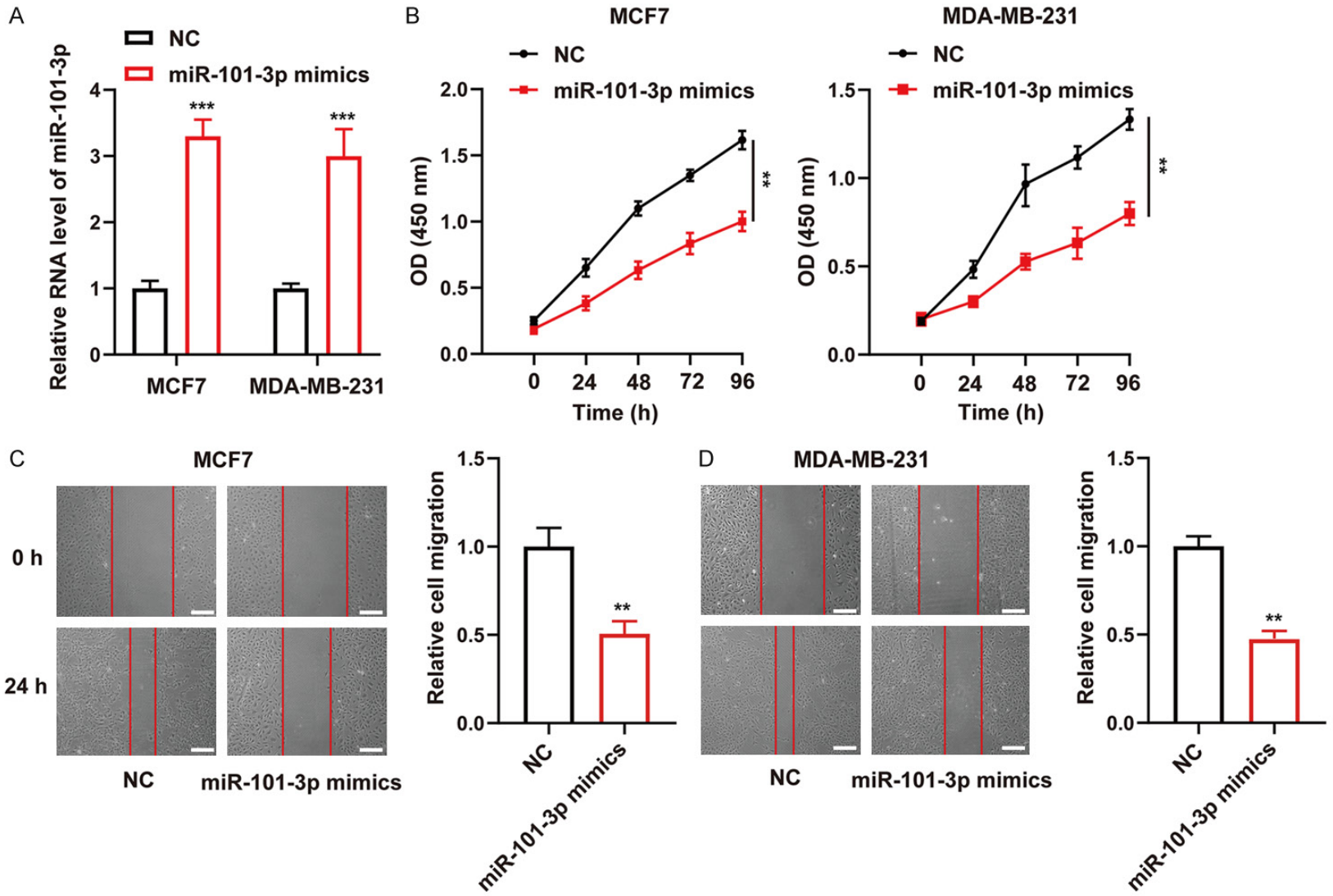
A
NC
miR-101-3p mimics
Relative RNA level of miR-101-3p
***
***
MCF7
MDA-MB-231
B
MCF7
NC
miR-101-3p mimics
OD (450 nm)
**
Time (h)
MDA-MB-231
NC
miR-101-3p mimics
OD (450 nm)
**
Time (h)
C
MCF7
0 h
24 h
NC
miR-101-3p mimics
Relative cell migration
**
NC
miR-101-3p mimics
D
MDA-MB-231
NC
miR-101-3p mimics
Relative cell migration
**
NC
miR-101-3p mimics

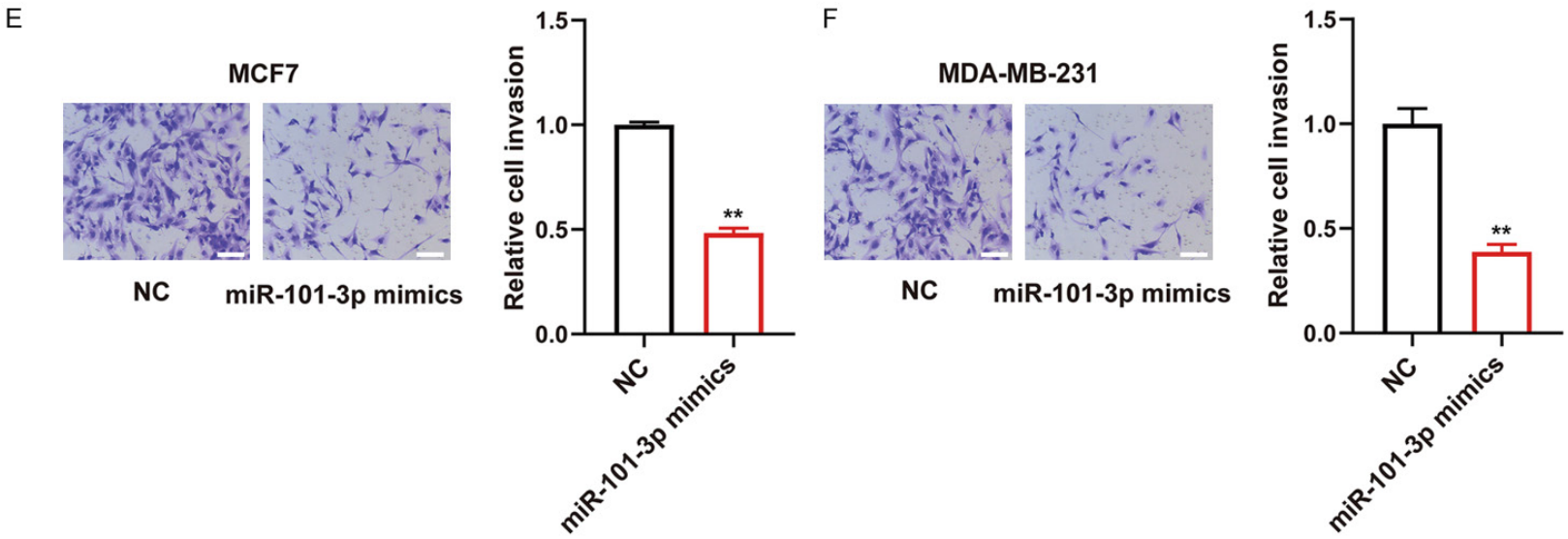

Figure 4. MiR-101-3p overexpression inhibits BC cell growth, invasion, and migration. MDA-MB-231 and MCF-7 cells subjected to NC or miR-101-3p mimic transfection for analysis. A. MiR-101-3p expression levels in the BC cells examined using qRT-PCR. B. BC cell proliferation measured using CCK8 assays. C and D. BC cell migration determined using scratch assays (scale bar = 500 μm, magnification × 40). E and F. BC cell invasion examined using transwell assays. (magnification × 200, scale bar = 100 μm). Compared to the NC group, $^{**}P < 0.01$, $^{***}P < 0.001$.

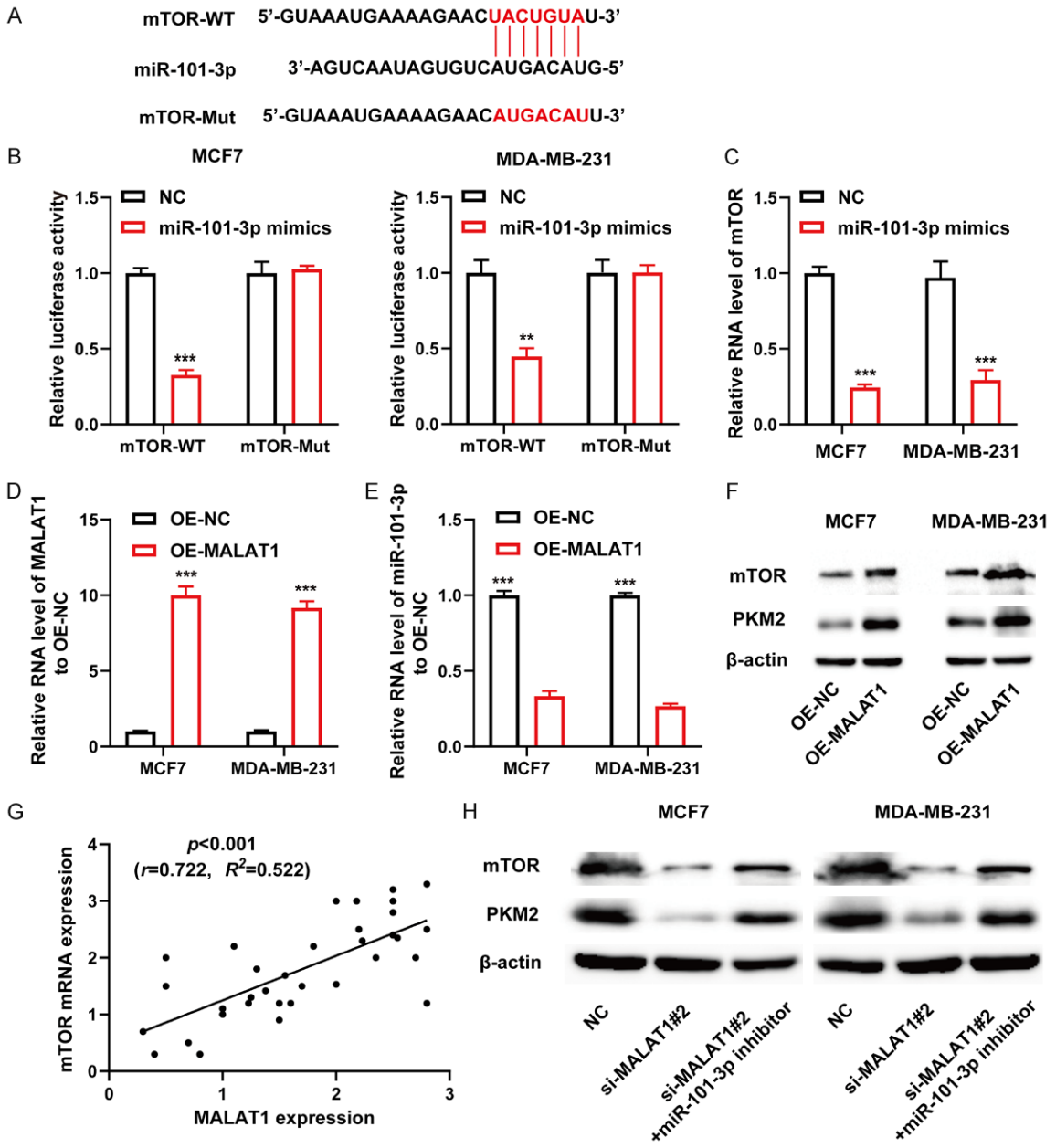

Figure 5. MALAT1 knockdown inhibits the mTOR/PKM2 pathway. (A) On the basis of mutating the miR-101-3p candidate binding site in mTOR, the luciferase reporter plasmids of mTOR-Mut and mTOR-WT were cloned. (B) BC cells cotransfected with luciferase reporter plasmids and NC or miR-101-3p mimics, and luciferase activities measured using dual-luciferase assays. (C) BC cells transfected with the NC or miR-101-3p mimics and assessing the mTOR expression in the cells using qRT-PCR. (D, E) pcDNA3.1-NC or pcDNA3. MALAT1 transfected into BC cells, and MALAT1 and miR-101-3p expression in the cells analyzed using qRT-PCR. (F) mTOR/PKM2 pathway expression performed using Western blot (G) Association of the MALAT1 level with the mTOR expression in the BC clinical samples identified using Spearman's correlation. (H) The mTOR/PKM2 pathway level in the BC cells assessed using Western blot, and the cells cotransfected with si-MALAT1#2, or si-MALAT1#2 and NC or an miR-101-3p inhibitor. Compared to the NC or OE-NC group, $^{**}P < 0.01$, $^{***}P < 0.001$.

cal activity of BC cells. The binding sites were present in miR-101-3p for the mTOR 3'-UTR region, as shown in **Figure 5A**. The miR-101-3p mimics reduced the luciferase activities of the BC cells subjected to an mTOR-WT transfection, but they did not significantly affect the activities of the BC cells transfected with mTOR-Mut (**Figure 5B**). The mTOR mRNA levels in the BC

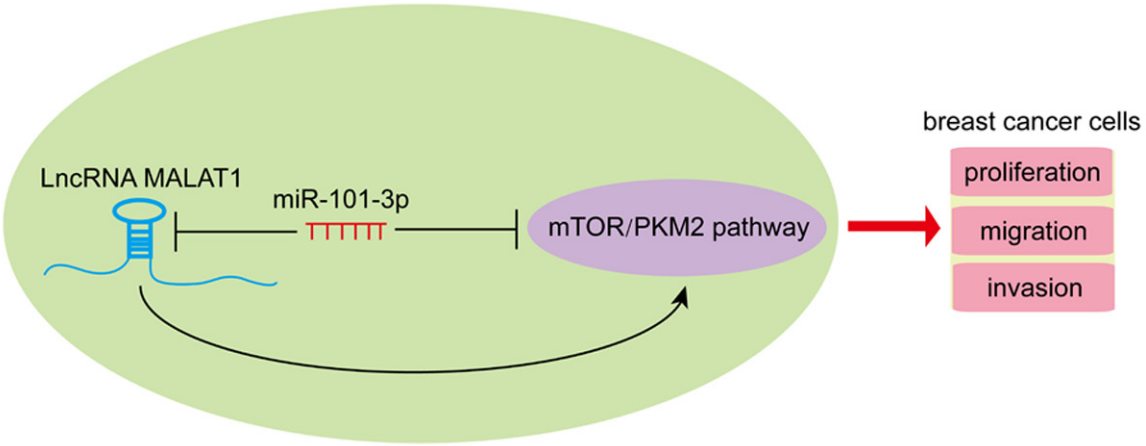

Figure 6. A schematic diagram of the mechanism regarding the lncRNA MALAT1/miR-101-3p axis in BC.

cells subjected to the miR-101-3p mimic transfection were significantly lower in the cells under NC-transfection (**Figure 5C**). Additionally, the effect of the MALAT1 overexpression was identified in the miR-101-3p expression, so the mTOR/PKM2 pathway is implicated in cancer cell development and survival [19-21]. The MALAT1 level was significantly upregulated in pcDNA3.1-MALAT1 compared with the MALAT1 levels in the MDA-MB-231 and MCF-7 cells in the OE-NC group (**Figure 5D**). Although the MALAT1 overexpression significantly inhibited the miR-101-3p level, it upregulated the mTOR and PKM2 protein levels (**Figure 5E** and **5F**). Furthermore, our Spearman's correlation showed that the MALAT1 expression is directly proportional to the mTOR level (**Figure 5G**), suggesting that MALAT1 can target miR-101-3p to regulate the mTOR level. The MALAT1 knockdown markedly reduced the mTOR and PKM2 expressions in the MDA-MB-231 and MCF-7 cells, but the miR-101-3p inhibitor reversed this effect (**Figure 5E**). Thus, MALAT1 can regulate the mTOR/PKM2 pathway in BC cells, and miR-101-3p might serve as a crucial mediator. A sketch map for the lncRNA MALAT1/miR-101-3p axis in BC is illustrated in **Figure 6**.

Discussion

BC has a marked female predilection globally. No substantive breakthrough in its diagnosis or treatment has been made due to its high heterogeneity, high proliferative ability, and tolerance to clinical treatment (such as chemotherapy and radiotherapy tolerance) [22, 23]. lncRNAs have vital functions during the development of complicated diseases, including BC [24]. MALAT1, a type of lncRNA, is related to tumor metastasis and development, which have been suggested to serve as an accurate diagnosis for BC [25]. Nonetheless, the mechanism by which MALAT1 promotes tumorigenesis in BC remains unclear. The present study found that MALAT1 expressions increase in BC cells and tissues, which leads to the dismal overall survival ratio. Moreover, our study found that MALAT1 knockdown may exert an inhibitory effect on BC cell proliferation, invasion, and migration by modulating the mTOR/PKM2 pathway by targeting miR101-3p.

MALAT1 can promote cancer cell growth, migration, metastasis, and invasion [26, 27], but a knockdown using antisense oligonucleotide or the genetic knockout of MALAT1 remarkably suppresses cancer cell growth, metastasis, and migration from the *in vitro* and *in vivo* models of lung cancer and BC [28, 29]. Additionally, MALAT1 promotes the progression of hepatocellular carcinoma by modulating Wnt pathway activation and inducing the oncogenic splicing factor, SRSF1 [30]. These studies agree with our findings in the BC cell lines. However, Kim et al. showed an opposite phenotype, suggesting that transgenic MALAT1 overexpression inhibits metastasis and cell migration in MMTV-PyMT mammary tumors [31]. Therefore, the roles of MALAT1 may vary according to the cancer type. As a competitive endogenous RNA (ceRNA), lncRNAs exhibit different biological functions in different cancers by targeting miRNAs [32]. The present study confirmed using an bioinformatics analysis and luciferase activ-

ity assays that miR-101-3p sponges MALAT1 in BC cells. Additionally, the miR-124-3p levels were indirectly proportional to the MALAT1 level in the BC samples.

The effect of miR-101-3p on BC cells was further explored by targeting miR-101-3p to determine the MALAT1 regulation during BC pathogenesis. Because miR-101-3p is associated with MALAT1-regulated BC development, we can conclude that miR-101-3p overexpression inhibits BC cell growth, invasion, and migration. Thus, MALAT1 acts as an oncogenic gene in BC partly by modulating miR-101-3p. Additionally, miR-101-3p might modulate several targets including mTOR. Conversely, miR-101-3p, the candidate intervention target, can reverse titanium dioxide nanoparticle (TiO2NP)-mediated human trophoblastic cell autophagy and the impaired migration by specifically reducing the mTOR expression [33]. PKM2 is one of the downstream targets of mTOR and is implicated in cancer cell survival and development [34]. The present study investigated whether MALAT1 could modulate the mTOR/PKM2 pathway in BC and explored the molecular mechanism of MALAT. MALAT1 overexpression significantly reduced the miR-101-3p expression and increased the mTOR/PKM2 pathway protein levels. Additionally, MALAT1 knockdown significantly reduced the mTOR/PKM2 pathway protein level, and this effect was inhibited using the miR-101-3p inhibitor. Thus, MALAT1 targets miR-101-3p and regulates BC progression by regulating the mTOR/PKM2 pathway.

MALAT1 can regulate BC progression including cell growth, invasion, and migration by downregulating the miR-101-3p level and miR-101-3p overexpression. Additionally, MALAT1 can promote the expression of the mTOR/PKM2 pathway, but the miR-101-3p level is negatively correlated with the mTOR expression. Thus, MALAT1 may regulate BC progression by upregulating the expression of the mTOR/PKM2 pathway through miR-101-3p sponging.

However, the present study could not provide experimental evidence in vivo. Additionally, further studies are required to investigate the effect of miR-101-3p on BC invasion and development and the function of miR-101-3p in regulating BC using the mTOR/PKM2 pathway.

Acknowledgements

This work was financially supported by the Medical Science Research Project of Hebei Province (No. 20200307).

Disclosure of conflict of interest

None.

Address correspondence to: Zunyi Wang, Department III of Thyroid & Breast, Cangzhou Central Hospital, No. 16 Xinhua West Road, Cangzhou 061000, Hebei, China. Tel: +86-13731708954; E-mail: wangzunyi01@163.com

References

[1] Harbeck N and Gnant MJL. Breast cancer. 2016; 16.

[2] Keklikoglou I, Cianciaruso C, Guc E, Squadrito ML, Spring LM, Tazzyman S, Lambein L, Poissonnier A, Ferraro GB, Baer C, Cassara A, Guichard A, Iruela-Arispe ML, Lewis CE, Coussens LM, Bardia A, Jain RK, Pollard JW and De Palma M. Chemotherapy elicits pro-metastatic extracellular vesicles in breast cancer models. Nat Cell Biol 2019; 21: 190-202.

[3] Shen M, Jiang YZ, Wei Y, Ell B, Sheng X, Esposito M, Kang J, Hang X, Zheng H, Rowicki M, Zhang L, Shih WJ, Celia-Terrassa T, Liu Y, Cristea I, Shao ZM and Kang Y. Tinagl1 suppresses triple-negative breast cancer progression and metastasis by simultaneously inhibiting integrin/FAK and EGFR signaling. Cancer Cell 2019; 35: 64-80, e67.

[4] Li Y, Song Y, Wang Z, Zhang Z, Lu M and Wang Y. Long non-coding RNA LINC01787 drives breast cancer progression via disrupting miR-125b generation. Front Oncol 2019; 9: 1140.

[5] DeSantis CE, Ma J, Goding Sauer A, Newman LA and Jemal A. Breast cancer statistics, 2017, racial disparity in mortality by state. CA Cancer J Clin 2017; 67: 439-448.

[6] Zhou L, Tian Y, Guo F, Yu B, Li J, Xu H and Su Z. LincRNA-p21 knockdown reversed tumor-associated macrophages function by promoting MDM2 to antagonize* p53 activation and alleviate breast cancer development. Cancer Immunol Immunother 2020; 69: 835-846.

[7] Iyer MK, Niknafs YS, Malik R, Singhal U, Sahu A, Hosono Y, Barrette TR, Prensner JR, Evans JR, Zhao S, Poliakov A, Cao X, Dhanasekaran SM, Wu YM, Robinson DR, Beer DG, Feng FY, Iyer HK and Chinnaiyan AM. The landscape of long noncoding RNAs in the human transcriptome. Nat Genet 2015; 47: 199-208.

[8] Huarte M. The emerging role of lncRNAs in cancer. Nat Med 2015; 21: 1253-1261.
[9] Vafadar A, Shabaninejad Z, Movahedpour A, Mohammadi S, Fathullahzadeh S, Mirzaei HR, Namdar A, Savardashtaki A and Mirzaei H. Long non-coding RNAs as epigenetic regulators in cancer. Curr Pharm Des 2019; 25: 3563-3577.
[10] Xu YH, Deng JL, Wang G and Zhu YS. Long noncoding RNAs in prostate cancer: functional roles and clinical implications. Cancer Lett 2019; 464: 37-55.
[11] Zhang TN, Goodwin JE, Liu B, Li D, Wen R, Yang N, Xia J, Zhou H, Zhang T, Song WL and Liu CF. Characterization of long noncoding RNA and mRNA profiles in sepsis-induced myocardial depression. Mol Ther Nucleic Acids 2019; 17: 852-866.
[12] Ji J, Xu R, Ding K, Bao G, Zhang X, Huang B, Wang X, Martinez A, Wang X, Li G, Miletic H, Thorsen F, Bjerkvig R, Xiang L, Han B, Chen A, Li X and Wang J. Long noncoding RNA SChLAP1 forms a growth-promoting complex with HNRNPL in human glioblastoma through stabilization of ACTN4 and activation of NF-kappaB signaling. Clin Cancer Res 2019; 25: 6868-6881.
[13] Ghosal S, Das S, Pang Y, Gonzales MK, Huynh TT, Yang Y, Taieb D, Crona J, Shankavaram UT and Pacak K. Long intergenic noncoding RNA profiles of pheochromocytoma and paraganglioma: a novel prognostic biomarker. Int J Cancer 2020; 146: 2326-2335.
[14] Sun Y and Ma L. New insights into long noncoding RNA MALAT1 in cancer and metastasis. Cancers (Basel) 2019; 11: 216.
[15] Yoshimoto R, Mayeda A, Yoshida M and Nakagawa S. MALAT1 long non-coding RNA in cancer. Biochim Biophys Acta 2016; 1859: 192-9.
[16] Zheng L, Zhang Y, Fu Y, Gong H, Guo J, Wu K, Jia Q and Ding X. Long non-coding RNA MALAT1 regulates BLCAP mRNA expression through binding to miR-339-5p and promotes poor prognosis in breast cancer. Biosci Rep 2019; 39: BSR20181284.
[17] Ji P, Diederichs S, Wang W, Boing S, Metzger R, Schneider PM, Tidow N, Brandt B, Buerger H, Bulk E, Thomas M, Berdel WE, Serve H and Muller-Tidow C. MALAT-1, a novel noncoding RNA, and thymosin beta4 predict metastasis and survival in early-stage non-small cell lung cancer. Oncogene 2003; 22: 8031-8041.
[18] Zidan HE, Karam RA, El-Seifi OS and Abd Elrahman TM. Circulating long non-coding RNA MALAT1 expression as molecular biomarker in Egyptian patients with breast cancer. Cancer Genet 2018; 220: 32-37.
[19] Dando I, Cordani M and Donadelli M. Mutant p53 and mTOR/PKM2 regulation in cancer cells. IUBMB Life 2016; 68: 722-726.
[20] Gao S, Chen M, Wei W, Zhang X, Zhang M, Yao Y, Lv Y, Ling T, Wang L and Zou X. Crosstalk of mTOR/PKM2 and STAT3/c-Myc signaling pathways regulate the energy metabolism and acidic microenvironment of gastric cancer. J Cell Biochem 2018; [Epub ahead of print].
[21] Li Z, Yang P and Li Z. The multifaceted regulation and functions of PKM2 in tumor progression. Biochim Biophys Acta 2014; 1846: 285-296.
[22] Benson JR and Jatoi I. The global breast cancer burden. Future Oncol 2012; 8: 697-702.
[23] Li Y, Zeng Q, Qiu J, Pang T, Xian J and Zhang X. Long non-coding RNA UCA1 promotes breast cancer by upregulating PTP1B expression via inhibiting miR-206. Cancer Cell Int 2019; 19: 275.
[24] Chen X and Yan GY. Novel human lncRNA-disease association inference based on lncRNA expression profiles. Bioinformatics 2013; 29: 2617-24.
[25] Zidan HE, Karam RA, El-Seifi OS and Abd Elrahman TM. Circulating long non-coding RNA MALAT1 expression as molecular biomarker in Egyptian patients with breast cancer. Cancer Genet 2018; 220: 32-37.
[26] Amodio N, Raimondi L, Juli G, Stamato MA, Caracciolo D, Tagliaferri P and Tassone P. MALAT1: a druggable long non-coding RNA for targeted anti-cancer approaches. J Hematol Oncol 2018; 11: 63.
[27] Zhang P, Zhou H, Lu K, Lu Y, Wang Y and Feng T. Exosome-mediated delivery of MALAT1 induces cell proliferation in breast cancer. Onco Targets Ther 2018; 11: 291-299.
[28] Arun G, Diermeier S, Akerman M, Chang KC, Wilkinson JE, Hearn S, Kim Y, MacLeod AR, Krainer AR, Norton L, Brogi E, Egeblad M and Spector DL. Differentiation of mammary tumors and reduction in metastasis upon Malat1 lncRNA loss. Genes Dev 2016; 30: 34-51.
[29] Gutschner T, Hammerle M, Eissmann M, Hsu J, Kim Y, Hung G, Revenko A, Arun G, Stentrup M, Gross M, Zornig M, MacLeod AR, Spector DL and Diederichs S. The noncoding RNA MALAT1 is a critical regulator of the metastasis phenotype of lung cancer cells. Cancer Res 2013; 73: 1180-1189.
[30] Malakar P, Shilo A, Mogilevsky A, Stein I, Pikarsky E, Nevo Y, Benyamini H, Elgavish S, Zong X, Prasanth KV and Karni R. Long noncoding RNA MALAT1 promotes hepatocellular carcinoma development by SRSF1 upregulation and mTOR activation. Cancer Res 2017; 77: 1155-1167.
[31] Kim J, Piao HL, Kim BJ, Yao F, Han Z, Wang Y, Xiao Z, Siverly AN, Lawhon SE, Ton BN, Lee H, Zhou Z, Gan B, Nakagawa S, Ellis MJ, Liang H, Hung MC, You MJ, Sun Y and Ma L. Long non-

coding RNA MALAT1 suppresses breast cancer metastasis. Nat Genet 2018; 50: 1705-1715.
[32] Abdollahzadeh R, Daraei A, Mansoori Y, Sepahvand M, Amoli MM and Tavakkoly-Bazzaz J. Competing endogenous RNA (ceRNA) cross talk and language in ceRNA regulatory networks: a new look at hallmarks of breast cancer. J Cell Physiol 2019; 234: 10080-10100.
[33] Mao Z, Yao M, Li Y, Fu Z, Li S, Zhang L, Zhou Z, Tang Q, Han X and Xia Y. miR-96-5p and miR-101-3p as potential intervention targets to rescue TiO2 NP-induced autophagy and migration impairment of human trophoblastic cells. Biomater Sci 2018; 6: 3273-3283.
[34] Goldberg MS and Sharp PA. Pyruvate kinase M2-specific siRNA induces apoptosis and tumor regression. J Exp Med 2012; 209: 217-224.